Available online at www.sciencedirect.com
SCIENCE DIRECT
Journal of Catalysis 231 (2005) 56–66
JOURNAL OF CATALYSIS
www.elsevier.com/locate/jcat

Following the evolution of iron from framework to extra-framework positions in isomorphously substituted [Fe,Al]MFI with ^{57}Fe Mössbauer spectroscopy

Jerome B. Taboada [a,*], Arian R. Overweg [a], Patricia J. Kooyman [b], Isabel W.C.E. Arends [c], Guido Mul [d]

[a] *Department of Radiation, Radionuclides and Reactors, Faculty of Applied Sciences, Delft University of Technology, Mekelweg 15, 2629 JB, Delft, The Netherlands*
[b] *DelftChemTech and National Centre for High Resolution Electron Microscopy, Delft University of Technology, Julianalaan 136, 2628 BL Delft, The Netherlands*
[c] *Section Biocatalysis and Organic Chemistry, Department of Biotechnology, Faculty of Applied Sciences, Delft University of Technology, Julianalaan 136, 2628 BL Delft, The Netherlands*
[d] *Reactor and Catalysis Engineering, DelftChemTech, Faculty of Applied Sciences, Delft University of Technology, Julianalaan 136, 2628 BL Delft, The Netherlands*

Received 3 November 2004; revised 23 December 2004; accepted 11 January 2005

Abstract

Isomorphously substituted [Fe,Al]MFI zeolites enriched with ^{57}Fe isotope were synthesized with varying iron (0.075–0.6 wt%) and aluminum (0–1.1 wt%) concentrations. The as-prepared zeolites underwent sequential post-treatment steps (i.e., calcination, transformation to H-form, and steam treatment), making them active in the one-step oxidation of benzene to phenol with N_2O as oxidant. Through ^{57}Fe Mössbauer spectroscopy, and transmission electron microscopy (TEM) as a complementary technique, we followed the evolution of the physico-chemical states of iron during the different post-treatment steps. In general, the extent to which iron is removed from framework to extra-framework positions, during different post-treatments, is higher for [Fe,Al]MFI zeolites containing high iron and aluminum concentrations. For all steamed [Fe,Al]MFI zeolites with an aluminum content of ~ 1.1 wt%, iron was predominantly present in the high-spin Fe^{2+} state (ca. 90% based on spectral contribution). This extraordinarily high concentration of Fe^{2+} species is significant, since the presence of Fe^{2+} was correlated to the formation of α-sites, which were reported to be responsible for the direct oxidation of benzene to phenol [1]. For [Fe,Al]MFI with less aluminum (~ 0.6 wt%), a mixture of Fe^{2+} (at least 30%) and Fe^{3+} ions was observed, whereas for the aluminum-free sample, only iron in the Fe^{3+} state was obtained.

Keywords: Steam-treated [Fe,Al]MFI; Extra-framework iron; Benzene to phenol; ^{57}Fe Mössbauer spectroscopy

1. Introduction

Iron-containing MFI-type zeolites, or [Fe,Al]MFI, have been widely used for many catalytic reactions, such as the selective catalytic reduction (SCR) of NO_x [2–5] and the direct decomposition of N_2O [6,7]. Recently they have attracted attention because of their use in the one-step oxidation of benzene to phenol with N_2O as oxidant [8–11]. Currently phenol is produced industrially via the three-step cumene process. However, this process has innate disadvantages (i.e., low efficiency in benzene consumption, the presence of a hazardous intermediate, and production of acetone in a 1:1 molar ratio), which makes a direct route of benzene oxidation to phenol more attractive. Panov and co-workers [8,9] were the first to report the remarkable catalytic activ-

* Corresponding author.
E-mail address: j.b.taboada@iri.tudelft.nl (J.B. Taboada).

0021-9517/$ – see front matter
doi:10.1016/j.jcat.2005.01.002

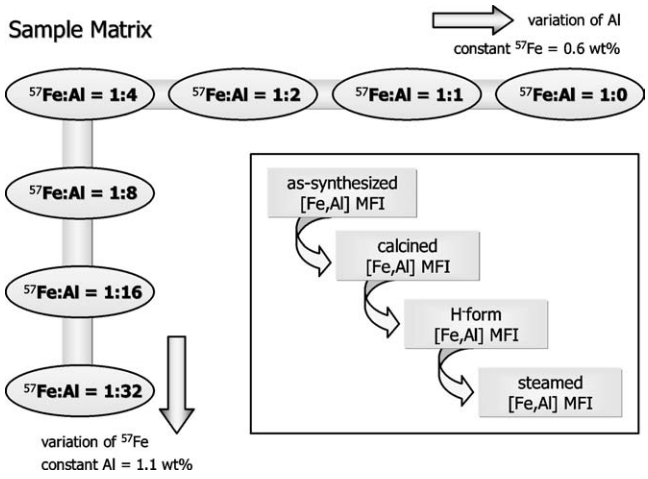

Fig. 1. Schematic representation of the sample matrix showing the variation of iron and aluminum concentrations. The inset shows the sequential post-treatment steps to activate the catalyst.

ity and selectivity of [Fe,Al]MFI in the one-step oxidation of benzene to phenol. They later ascribed the catalytic performance of [Fe,Al]MFI to extra-framework iron complexes stabilized in the zeolite channels, generating a new form of surface oxygen (α-oxygen) from N_2O [12].

Following the pioneering work of Panov and co-workers, some of us reported [11] the catalytic performance of [Fe,Al]MFI prepared by hydrothermal synthesis of isomorphously substituted [Fe,Al]MFI followed by calcination and subsequent treatment by steam at 873 K. This catalyst proves to be active in the direct oxidation of benzene to phenol with a selectivity of $>$ 99% and phenol yields up to 27%. A detailed physico-chemical characterization of this catalyst reveals a broad distribution of extra-framework iron species ranging from isolated mononuclear iron to large ($\sim$ 2 nm) iron oxide particles [13]. Although the catalytic properties of steamed [Fe,Al]MFI are well established, the structure and nature of the active site remain unclear. This is mainly due to the diversities in synthesis route, the chemical composition, and post-treatment conditions that further complicate the debate on the nature of the active site of the catalyst.

In this study, we systematically varied the iron and aluminum concentrations in the MFI zeolite, using lower iron concentration to prevent the formation of large iron oxide particles, which are known to be inactive in benzene-to-phenol; we also varied the aluminum concentration to study its influence on the formation of various iron sites. The as-prepared zeolites underwent sequential post-treatment steps (i.e., calcination, transformation to H-form, and steam treatment), making them active in the one-step oxidation of benzene to phenol. Fig. 1 shows the schematic of the sample variation and the post-treatment steps. The different post-treatment steps have previously been shown to cause the migration of iron from framework to extra-framework positions, creating various iron sites. Using ^{57}Fe Mössbauer spectroscopy, we probed the evolution of the physicochemical states of iron during the different post-treatment steps. ^{57}Fe Mössbauer spectroscopy is the ideal method for the study of the valence, coordination, and magnetic properties of the iron species in the [Fe,Al]MFI catalyst because, unlike in electron paramagnetic resonance (EPR), there is no form of iron that is Mössbauer-silent. Moreover, the observed spectrum is the sum of different subspectra corresponding to iron in different environments, thus providing richer information compared with bulk-averaging techniques such as magnetic susceptibility.

^{57}Fe Mössbauer spectroscopy is based on the recoilless emission and absorption of γ-ray photons. The resonance window (i.e., the Mössbauer effect) has a very high energy resolution that enables us to measure the hyperfine interactions [14], which provide chemical and structural information for a sample. Three important hyperfine interactions measured in a Mössbauer spectrum are (1) isomer shift, which indicates the oxidation state; (2) the quadrupole interaction, which is a measure of the symmetry distortion, and thus the coordination state; and (3) the magnetic hyperfine interaction, which renders the magnetic properties of the sample.

Iron concentrations were systematically varied; the highest was 0.6 wt%. This amount appears to be the limit at which iron can be isomorphously incorporated into the MFI framework [15]. Because of low iron loading (0.075–0.6 wt%) of the samples, we enriched the zeolite with iron isotope ^{57}Fe to render it more sensitive to ^{57}Fe Mössbauer spectroscopy. Aluminum concentrations were also varied from $\sim$ 1.1 wt% (as with most [Fe,Al]MFI) to no aluminum (i.e., Fe-silicalite).

2. Experimental

2.1. Preparation of [Fe,Al]MFI

Isomorphously substituted [Fe,Al]MFI zeolites enriched with ^{57}Fe isotope were prepared by hydrothermal synthesis with varying iron (0.075–0.6 wt%) and aluminum (0–1.1 wt%) concentrations, which was described in a previous publication [15]. There we mentioned that rotation of the autoclave during hydrothermal treatment is crucial in obtaining [Fe,Al]MFI zeolites containing iron and aluminum concentrations similar to those of the starting solution gel. This is important specifically in the preparation of a set of zeolites where there is a systematic variation of the iron and aluminum concentrations in the MFI structure. Table 1 gives a summary of all as-prepared samples with their corresponding molar ratio both in the synthesis gel and in the zeolite crystal. To remove the organic template in the as-prepared zeolites, the samples were calcined in static air at 823 K for 10 h. The calcined zeolites were then transformed into the H-form by three consecutive exchanges with 0.1 M ammonium nitrate overnight and subsequent calcination at 823 K for 5 h. Finally, the samples were heated to 873 K in 30 ml min^{-1} of He and steamed (water partial pressure of

Table 1
ICP-OES results of the *as*-synthesized FeMFI zeolites

Sample	Si (wt%)[a]	Al (wt%)[a]	Fe (wt%)[a]	Si/Al (mol mol^{-1})[b]	Si/Fe (mol mol^{-1})[b]	Si/Al (mol mol^{-1})[c]	Si/Fe (mol mol^{-1})[c]
[Fe,Al]MFI (1:32)$_{as}$	39.0	1.2	0.08	31	1018	36	1200
[Fe,Al]MFI (1:16)$_{as}$	39.0	1.15	0.14	33	558	36	600
[Fe,Al]MFI (1:8)$_{as}$	39.0	1.16	0.28	33	279	36	300
[Fe,Al]MFI (1:4)$_{as}$[d]	39.0	1.1	0.56	33	141	36	152
[Fe,Al]MFI (1:2)$_{as}$	40.0	0.63	0.60	62	135	70	152
[Fe,Al]MFI (1:1)$_{as}$	41.0	0.22	0.47	176	175	152	152
[Fe,Al]MFI (1:0)$_{as}$	39.7	–	0.5	–	154	–	152

[a] Weight percent in the crystalline samples.
[b] Molar ratio of the crystalline samples.
[c] Molar ratio of the solution gel.
[d] Used as reference sample in the systematic variation of iron and aluminum concentrations.

300 mbar and 30 ml min^{-1} of He flow) at the same temperature for 5 h, making them active in the one-step oxidation of benzene to phenol with N_2O as oxidant. For all samples, calcination and steam-treatment steps were carried out with a temperature ramp of 5 K min^{-1}.

2.2. Characterization techniques

The elemental analysis of the as-prepared zeolites was carried out by inductively coupled plasma optical emission spectroscopy (ICP-OES) (Perkin–Elmer Plasma 40 (Si) and Optima 3000DV (axial)).

Transmission electron microscopy (TEM) was performed with a Philips CM30UT electron microscope with a field emission gun as the source of electrons operated at 300 kV. We mounted samples on Quantifoil carbon polymer supported on a copper or gold grid by placing a few droplets of a suspension of ground sample in ethanol on the grid; this was followed by drying at ambient conditions.

^{57}Fe Mössbauer spectra were measured on a constant-acceleration spectrometer in a triangular mode with a ^{57}Co:Rh source. Spectra for the different [Fe,Al]MFI samples were obtained at 300 K (both in air and in high vacuum, 10^{-6} mbar), and 77 K and 4.2 K in high vacuum. The spectra were fitted with Lorentzian-shaped lines to obtain the Mössbauer parameters (i.e., isomer shift [IS], quadrupole splitting [QS], and hyperfine field [HF]). Isomer shift values are reported relative to sodium nitroprusside. The magnetically split lines were fitted with several components to simulate a distribution of hyperfine fields. Thus, the hyperfine field reported here is the average value.

3. Results

A summary of the ICP-OES results for the as-prepared [Fe,Al]MFI zeolites is given in Table 1. For all samples, the relative molar concentrations of silicon, aluminum, and iron in the zeolite crystal are comparable to those in the solution gel. X-ray diffractograms of these materials (not shown) affirm that all have the MFI-type zeolite topology with a high degree of crystallinity. These results suggest that we have successfully synthesized [Fe,Al]MFI zeolites with the appropriate variations in iron and aluminum concentrations. For discussion purposes, the as-prepared, calcined, H-form, and steamed [Fe,Al]MFI samples are denoted by the subscripts *as*, *cal*, *H*, and *stm*, respectively, and the given ratio in parentheses indicates the relative molar ratio of iron to aluminum (see Table 1).

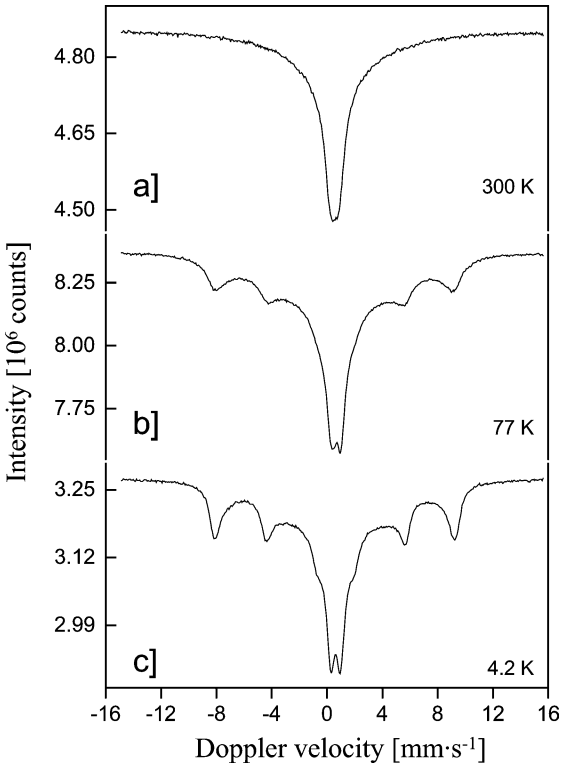

Fig. 2. ^{57}Fe Mössbauer spectra of [Fe,Al]MFI (1:4)$_{as}$ taken at (a) 300 K in air, (b) 77 K in 10^{-6} mbar vacuum, and (c) 4.2 K in 10^{-6} mbar vacuum.

3.1. As-prepared [Fe,Al]MFI zeolites

The Mössbauer spectrum of [Fe,Al]MFI (1:4)$_{as}$ at 300 K in air (Fig. 2a) exhibits a broad singlet with an isomer shift of 0.52 mm s^{-1}. This indicates the presence of tetrahedrally

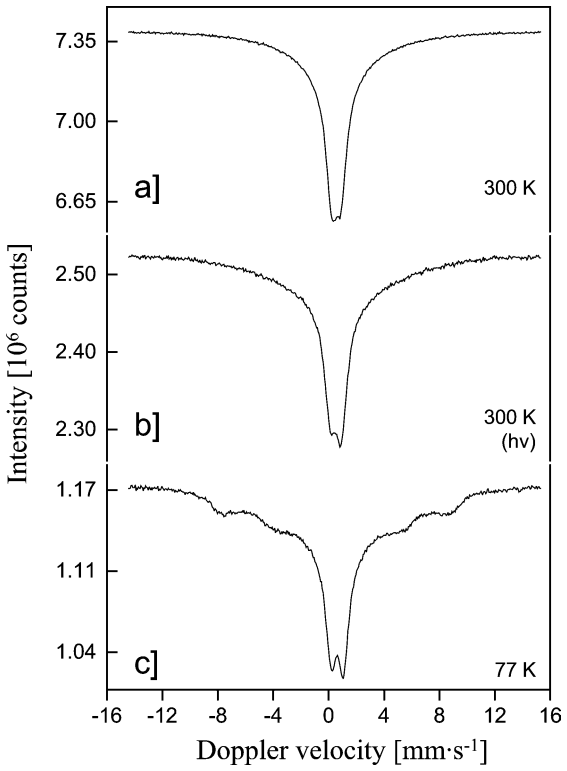

Fig. 3. ^{57}Fe Mössbauer spectra of [Fe,Al]MFI $(1{:}4)_{cal}$ taken at (a) 300 K in air, (b) 300 K in 10^{-6} mbar vacuum (*hv*), and (c) 77 K in 10^{-6} mbar vacuum.

Table 2
^{57}Fe Mössbauer hyperfine parameters and relative intensities for FeMFI (4:1) at different treatments

Spectrum[a]	[IS] ($mm\,s^{-1}$)	[QS] ($mm\,s^{-1}$)	[HF] (T)	Relative intensity (%)	Oxidation state
2a	0.52			100	Fe^{3+}
2b	0.59			34	Fe^{3+}
	0.59	0.69		11	Fe^{3+}
	0.59		53.1	55	Fe^{3+}
2c	0.61			29	Fe^{3+}
	0.61	0.72		10	Fe^{3+}
	0.61		53.7	61	Fe^{3+}
3a	0.54	0.662		41	Fe^{3+}
	0.54			59	Fe^{3+}
3b	0.54	0.874		34	Fe^{3+}
	0.58			66	Fe^{3+}
3c	0.62	0.91		17	Fe^{3+}
	0.66		49.2	83	Fe^{3+}
6a	0.67	0.96		24	Fe^{3+}
	0.54			76	Fe^{3+}
6b	0.61	1.09		56	Fe^{3+}
	1.30	2.75		6	Fe^{2+}
	0.54			38	Fe^{3+}
6c	0.69	1.26		44	Fe^{3+}
	1.68	2.95		7	Fe^{2+}
	0.77		49.8	49	Fe^{3+}

[a] Spectrum numbers correspond to the numbers of their respective figures.

coordinated high-spin Fe^{3+} ions [16,17], affirming the incorporation of iron into the MFI zeolite framework. The broad singlet is typical of paramagnetic Fe^{3+} ions with slow electron spin relaxation. At low temperatures (Fig. 2b and 2c), the broad component in the spectra at 300 K resolves into a six-line pattern (sextuplet) with a maximum hyperfine field of 53.1 T at 77 K and 53.7 T at 4.2 K. The presence of the hyperfine field at low temperatures is attributed to paramagnetic hyperfine splitting [18] and suggests large Fe–Fe distances typical for homogeneously well-distributed Fe^{3+} ions. The spectra at 77 K and 4.2 K were fitted with three components corresponding to the three Kramers' doublets ($S_z = \pm 5/2, \pm 3/2, \pm 1/2$) for high-spin Fe^{3+} with different electron spin relaxation times (τ_R).

The Mössbauer spectra for the other as-prepared [Fe,Al]MFI zeolites are comparable to those for [Fe,Al]MFI $(1{:}4)_{as}$ (not shown for brevity). All spectra show a broad singlet at 300 K with an isomer shift close to 0.52 $mm\,s^{-1}$. This indicates that iron in all as-prepared zeolites is present as ferric (Fe^{3+}) ions that are tetrahedrally coordinated in the MFI framework and are homogeneously well distributed.

3.2. Calcined [Fe,Al]MFI zeolites

Calcination of the [Fe,Al]MFI $(1{:}4)_{as}$ to remove the template results in small but significant changes in the zeolite structure, as shown in the Mössbauer spectra (see Fig. 3). The Mössbauer spectrum of [Fe,Al]MFI $(1{:}4)_{cal}$ taken at 300 K in air (Fig. 3a) shows a slightly broadened peak compared with the spectrum of the as-prepared sample recorded under the same conditions. The presence of an unresolved doublet indicates that a fraction of iron ions in [Fe,Al]MFI $(1{:}4)_{cal}$ is exhibiting a faster electron relaxation time due to an enhanced spin–spin interaction between Fe ions as a result of reduced Fe–Fe ion distances. This suggests that a fraction of framework iron has migrated to extra-framework positions during calcination, allowing it to move freely and closer to other iron ions, in both the framework and extra-framework positions.

Under high-vacuum (10^{-6} mbar) conditions, the doublet becomes more pronounced, as shown in Fig. 3b, and an increase in the quadrupole splitting of the doublet from 0.66 $mm\,s^{-1}$ (recorded in air) to 0.87 $mm\,s^{-1}$ is observed (see Table 2). The increased contribution of this doublet has been interpreted as being due to an increased interaction of the extra-framework Fe^{3+} to the zeolite lattice. Evacuation to high-vacuum conditions leads to the removal of physisorbed water (since all samples were unavoidably exposed to air after calcination for considerable time, i.e., days to weeks) from the zeolite pores, which will give rise to an increased electrostatic interaction between the positively charged ferric ions and the negatively charged zeolite lattice. The increased interaction between extra-framework ferric ions and the zeolite lattice results in an increased recoil-free fraction of this component, as evident from an increase in total resonant absorption area from 6.6 to 7.0 units.

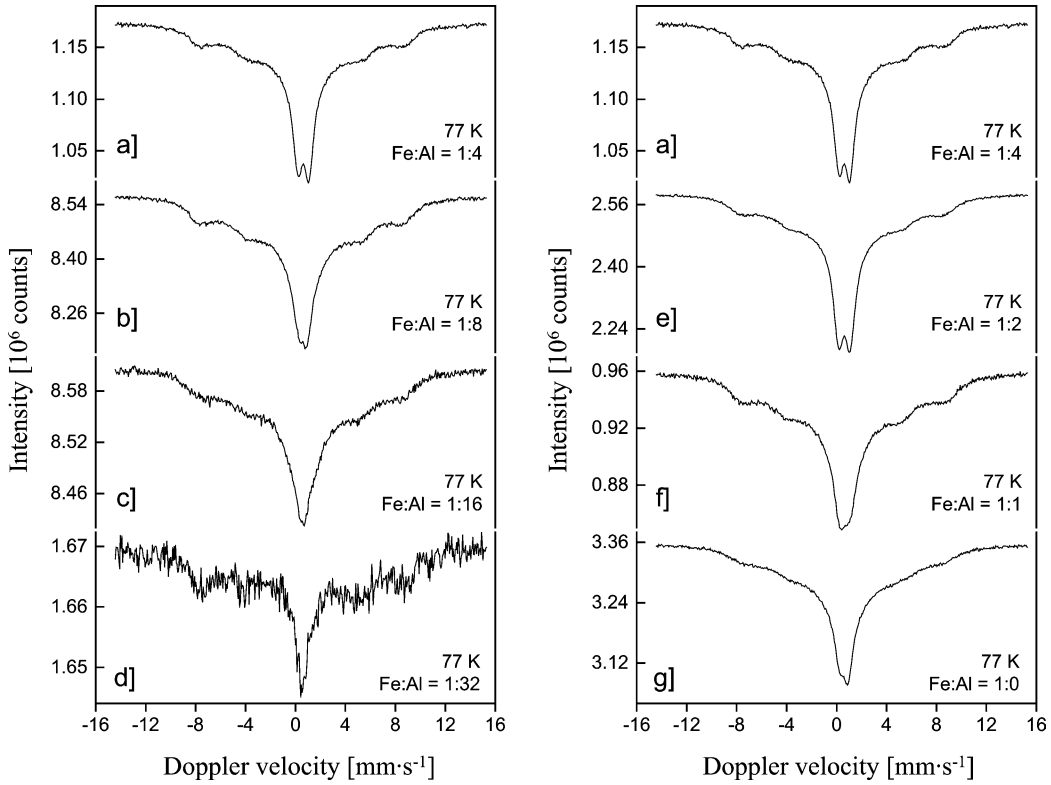

Fig. 4. ^{57}Fe Mössbauer spectra of (a) [Fe,Al]MFI (1:4)$_{cal}$, (b) [Fe,Al]MFI (1:8)$_{cal}$, (c) [Fe,Al]MFI (1:16)$_{cal}$, (d) [Fe,Al]MFI (1:32)$_{cal}$, (e) [Fe,Al]MFI (1:2)$_{cal}$, (f) [Fe,Al]MFI (1:1)$_{cal}$, and (g) [Fe,Al]MFI (1:0)$_{cal}$, taken at 77 K in 10^{-6} mbar vacuum.

At 77 K (Fig. 3c), the Mössbauer spectrum exhibits a well-resolved doublet and a broad, magnetically split component. The doublet has an isomer shift of 0.62 mm s^{-1} and a quadrupole splitting of 0.91 mm s^{-1}. Based on literature data [16,17], we attribute the doublet to octahedrally coordinated extra-framework Fe^{3+} ions in the high-spin state. The presence of a broad magnetic component at 77 K is most likely due to paramagnetic hyperfine splitting of isolated Fe^{3+} ions. The other possibility, the presence of very small iron oxide particles just below the superparamagnetic blocking temperature [19], was ruled out because of the absence of a superparamagnetic high-spin Fe^{3+} doublet at ambient conditions. This was further confirmed by TEM, which did not reveal any traces of any iron oxide-related phase (i.e., for [Fe,Al]MFI (1:4)$_{cal}$ and for the rest of the other calcined samples). In addition, the broad magnetic component has a hyperfine field of 49.2 T, which is lower compared with the value obtained for the as-prepared zeolite (53.1 T). This is explained by an increased relaxation due to reduced paramagnetic Fe–Fe ion distances, further affirming the removal of a fraction of the paramagnetic iron in the framework position to extra-framework iron species.

The spectral characteristics discussed above were also observed for samples with varying iron and aluminum concentrations. When their corresponding spectra at 77 K are plotted together (Fig. 4), we observe an increase in the intensity ratio of the quadrupole doublet to the broad magnetic component, and an increase in the quadrupole splitting, when both iron and aluminum concentrations are increased. Fig. 5 shows the increase in the intensity ratio of the high-spin Fe^{3+} doublet to the broad magnetic component, together with the increase in quadrupole splitting as a function of iron and aluminum concentrations. These suggest that iron is most likely to migrate from framework to extra-framework positions during calcination if the framework iron concentration is high, and in the presence of aluminum.

3.3. H-form [Fe,Al]MFI zeolites

For the [Fe,Al]MFI (1:4)$_H$, the Mössbauer spectrum taken at 300 K in air (Fig. 6a) shows a broad asymmetrical doublet that is fitted with two components: a quadrupole doublet and a broad component. Based on spectral parameters (see Table 2), the quadrupole doublet is attributed to octahedrally coordinated Fe^{3+} ions. This indicates that at least a quarter of the iron in the [Fe,Al]MFI (1:4)$_H$ has migrated from tetrahedrally coordinated framework to octahedrally coordinated extra-framework positions. The broad component, which partially resolves into a magnetically split component at low temperature (77 K), is attributed to paramagnetic isolated Fe^{3+} ions most likely in both framework and extra-framework positions.

At 300 K under high-vacuum conditions (Fig. 6b), the Mössbauer spectrum shows a well-resolved doublet with an increased quadrupole splitting. Similar to the situation of the calcined zeolites (vide supra), but much more prominent

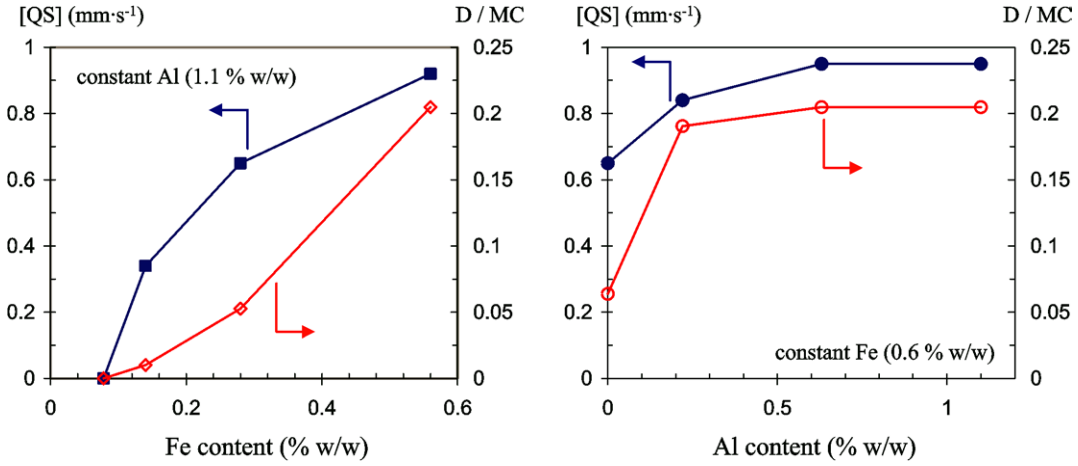

Fig. 5. Relative increase in quadrupole splitting and the intensity ratio of the quadrupole doublet to the magnetic component (D/MC) as a function of iron and aluminum concentrations.

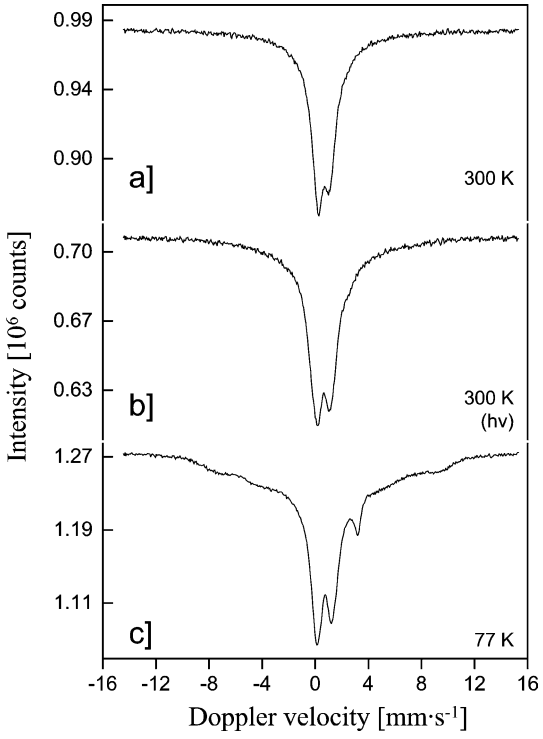

Fig. 6. ^{57}Fe Mössbauer spectra of [Fe,Al]MFI $(1{:}4)_H$ taken at (a) 300 K in air, (b) 300 K in 10^{-6} mbar vacuum (*hv*), and (c) 77 K in 10^{-6} mbar vacuum.

here, evacuation to high-vacuum condition leads to (1) an increase in the recoil-free fraction of the extra-framework Fe^{3+} ions due to the removal of physisorbed water (as evident from the increase in total resonant absorption area from 6.45 to 8.49 units) and (2) a further increase in the electron spin-relaxation rate due to the proximity of neighboring Fe^{3+} ions. In addition, because of the increase in the recoil-free fraction a weak shoulder is observed at the high-energy side of this doublet that is fitted with a second doublet with IS = 1.30 mm s^{-1} and QS = 2.75 mm s^{-1}. The spectral parameters of this second doublet suggest that a small part of iron in [Fe,Al]MFI $(1{:}4)_H$ is present as high-spin Fe^{2+} ions (6% based on the spectral fitting shown in table).

At 77 K (Fig. 6c), the spectrum is composed of a better-resolved high-spin Fe^{2+} doublet together with the high-spin Fe^{3+} doublet and a broad, magnetically split component. The high-spin Fe^{2+} and the high-spin Fe^{3+} doublets are both attributed to extra-framework iron species. It has been known that framework iron is difficult to reduce [20], and therefore Fe^{2+} ions are most likely in extra-framework positions. For the high-spin Fe^{3+} doublet, the spectral parameters indicate octahedrally coordinated ferric ions, and thus the ions are in extra-framework sites, since framework iron ions are tetrahedrally coordinated. The broad magnetic component with a hyperfine field of 49.8 T is attributed to paramagnetic hyperfine splitting of isolated ferric ions in both framework and extra-framework sites. Similar to the calcined samples, the presence of a magnetic component at 77 K could not be due to small iron oxide particles, since no traces of them were observed by TEM for all H-form samples.

For samples with varying iron concentration (see Fig. 7a–7d), the spectral contribution of the high-spin Fe^{3+} doublet is largest for [Fe,Al]MFI $(1{:}4)_H$, indicating the highest degree of clustering of extra-framework iron to small oligonuclear or oxo-Fe-species, as expected for samples with high iron concentration. However, for ferrous ions, the relative intensity of the high-spin Fe^{2+} doublet appears to have an optimum with a decrease in iron concentration (see also Table 3). Moreover, the intensity of the spectral contribution of the high-spin Fe^{2+} doublet diminishes with the decrease in aluminum concentration (see Fig. 7a and 7e–7g) and is evidently not observed in the [Fe,Al]MFI $(1{:}4)_H$ sample that does not contain aluminum.

3.4. Steamed [Fe,Al]MFI zeolites

For the samples with varying iron content, steam treatment leads to [Fe,Al]MFI catalysts that contain Fe^{2+} ions

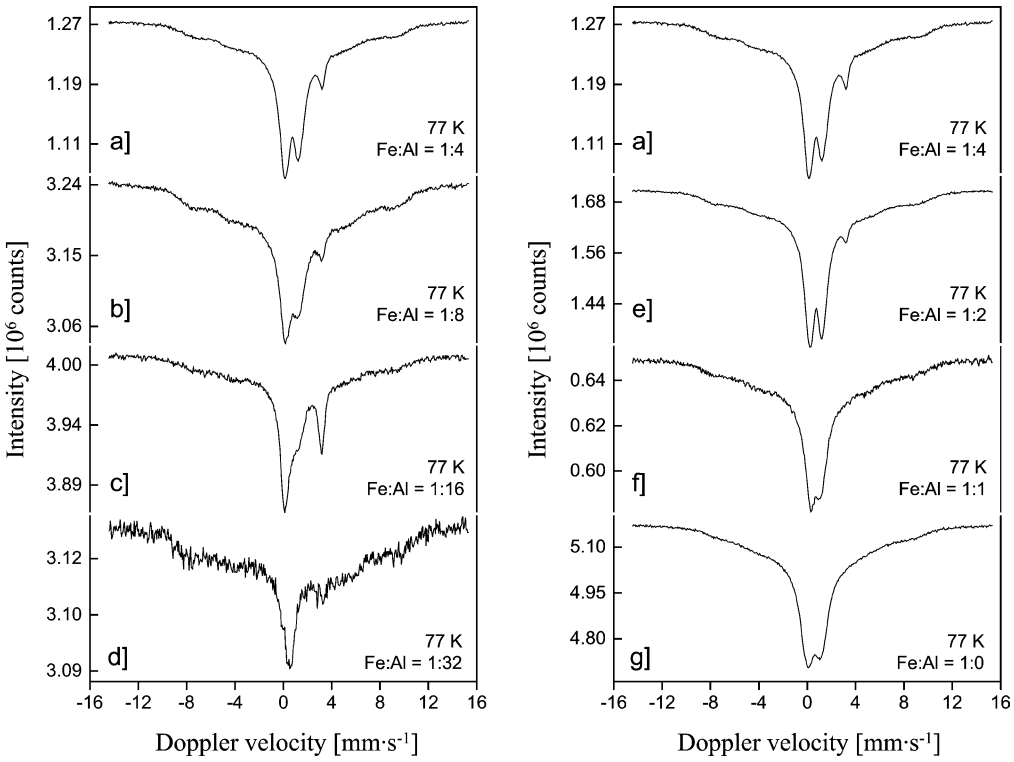

Fig. 7. ^{57}Fe Mössbauer spectra of (a) [Fe,Al]MFI (1:4)$_H$, (b) [Fe,Al]MFI (1:8)$_H$, (c) [Fe,Al]MFI (1:16)$_H$, (d) [Fe,Al]MFI (1:32)$_H$, (e) [Fe,Al]MFI (1:2)$_H$, (f) [Fe,Al]MFI (1:1)$_H$, and (g) [Fe,Al]MFI (1:0)$_H$, taken at 77 K in 10^{-6} mbar vacuum.

Table 3
^{57}Fe Mössbauer hyperfine parameters and relative intensities for spectra in Fig. 7

Spectrum[a]	[IS] (mm s^{-1})	[QS] (mm s^{-1})	[HF] (T)	Relative intensity (%)	Oxidation state
7a	0.69	1.26		44	Fe^{3+}
	1.68	2.95		7	Fe^{2+}
	0.77		49.8	49	Fe^{3+}
7b	0.74	1.17		34	Fe^{3+}
	1.64	2.99		8	Fe^{2+}
	0.85		51.4	58	Fe^{3+}
7c	0.70	1.00		35	Fe^{3+}
	1.62	3.06		20	Fe^{2+}
	0.87		49.6	45	Fe^{3+}
7d	0.54			15	Fe^{3+}
	1.60	3.20		5	Fe^{2+}
	0.77		52.2	80	Fe^{3+}
7e	0.71	1.14		45	Fe^{3+}
	1.75	2.82		5	Fe^{2+}
	0.72		51.0	50	Fe^{3+}
7f	0.56			30	Fe^{3+}
	0.75	0.95		18	Fe^{3+}
	0.68		47.7	52	Fe^{3+}
7g	0.57	1.24		51	Fe^{3+}
	0.66			49	Fe^{3+}

[a] Spectrum numbers correspond to the numbers of their respective figures.

exclusively (see Fig. 8a–8d) independent of iron concentration (i.e., < 0.6 wt% with constant 1.1 wt% aluminum). All spectra were fitted by a high-spin Fe^{2+} doublet (IS = 1.67 mm s^{-1}, QS = 3.19 mm s^{-1}), that is, ca. 90% based on spectral contribution (see Table 4).

Although steam treatment of [Fe,Al]MFI with varying iron concentration leads to the formation of extra-framework iron in the divalent state, steam treatment of [Fe,Al]MFI with varying aluminum reveals a distinct influence of aluminum on the oxidation state of iron. Figs. 8a and 8e–8g show the spectra of [Fe,Al]MFI (1:4)$_{stm}$, [Fe,Al]MFI (1:2)$_{stm}$, [Fe,Al]MFI (1:1)$_{stm}$, and [Fe,Al]MFI (1:0)$_{stm}$, respectively, taken at 4.2 K. As described above, [Fe,Al]MFI (1:4)$_{stm}$, containing the highest amount of aluminum among the series, is mainly characterized by a high-spin Fe^{2+} doublet. For [Fe,Al]MFI (1:2)$_{stm}$, containing roughly 50% less aluminum, the spectrum is a mixture of a high-spin Fe^{2+} doublet (IS = 1.66 mm s^{-1}, QS = 3.26 mm s^{-1}), a high-spin Fe^{3+} doublet (IS = 0.88 mm s^{-1}, QS = 0.92 mm s^{-1}), and a broad magnetic component with a hyperfine field of 50.1 T. The spectral contribution of the divalent iron decreases even further when the aluminum content in [Fe,Al]MFI (1:1)$_{stm}$ is lowered. However, it is worth mentioning that this spectrum (Fig. 8f) generates a complicated magnetic part of the spectrum that is not fully understood at the moment. To extract the spectral contribution of the high-spin Fe^{2+} doublet, the spectrum was fitted with several magnetic components (which may not have any physical significance); only the outermost hyperfine field value is reported in Table 4. For [Fe,Al]MFI (1:0)$_{stm}$ containing no aluminum, only contributions from Fe^{3+} ions were observed together with a broad sextuplet with a hyperfine field of 51.4 T. Based on spec-

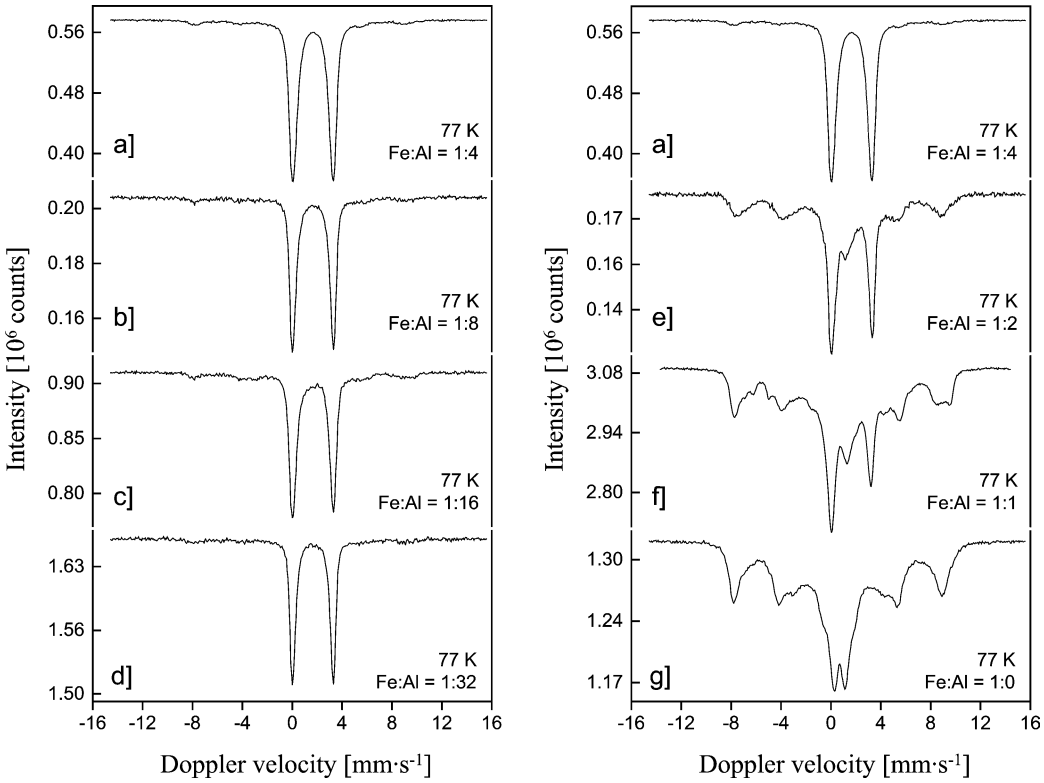

Fig. 8. ^{57}Fe Mössbauer spectra of (a) [Fe,Al]MFI (1:4)$_{stm}$, (b) [Fe,Al]MFI (1:8)$_{stm}$, (c) [Fe,Al]MFI (1:16)$_{stm}$, (d) [Fe,Al]MFI (1:32)$_{stm}$, (e) [Fe,Al]MFI (1:2)$_{stm}$, (f) [Fe,Al]MFI (1:1)$_{stm}$, and (g) [Fe,Al]MFI (1:0)$_{stm}$, taken at 4.2 K in 10^{-6} mbar vacuum.

Table 4
^{57}Fe Mössbauer hyperfine parameters and relative intensities for steam-treated samples in Fig. 8

Spectrum[a]	[IS] (mm s^{-1})	[QS] (mm s^{-1})	[HF] (T)	Relative intensity (%)	Oxidation state
8a	1.67	3.19		92	Fe^{2+}
	0.96		52.1	8	Fe^{3+}
8b	1.67	3.24		90	Fe^{2+}
	0.98		52.0	10	Fe^{3+}
8c	1.67	3.23		83	Fe^{2+}
	0.92		52.0	17	Fe^{3+}
8d	1.65	3.24		95	Fe^{2+}
	0.92		52.0	5	Fe^{3+}
8e	0.88	0.92		16	Fe^{3+}
	1.66	3.26		37	Fe^{2+}
	0.66		50.1	47	Fe^{3+}
8f	0.67	1.39		23	Fe^{3+}
	1.63	3.15		18	Fe^{2+}
	0.60		51.0	59	Fe^{3+}
8e	0.69	0.94		25	Fe^{3+}
	0.64		51.4	75	Fe^{3+}

[a] Spectrum numbers correspond to the numbers of their respective figures.

tral contributions, the amount of Fe^{2+} decreases from 92% in [Fe,Al]MFI (1:4)$_{stm}$ to 37% in [Fe,Al]MFI (1:2)$_{stm}$, 18% in [Fe,Al]MFI (1:1)$_{stm}$, and 0% in [Fe,Al]MFI (1:0)$_{stm}$.

TEM shows that no large Fe oxide particles are present in any steamed sample, as evident from the absence of any iron-related phase at high magnification (see Fig. 9). For the steamed samples with varying aluminum concentration, the absence of any traces of iron oxide particles by TEM indicates that the presence of a magnetically split component with an average hyperfine field of 51 T at 4.2 K is due to paramagnetic hyperfine splitting of isolated extra-framework Fe^{3+} ions. This is also confirmed by our Mössbauer measurements with an applied external magnetic field, where paramagnetic hyperfine splitting was observed, rather than magnetic behavior of superparamagnetic iron oxide particles.

4. Discussion

4.1. As-prepared to calcined [Fe,Al]MFI zeolites

For all as-synthesized [Fe,Al]MFI zeolites with varying iron and aluminum concentrations, Mössbauer spectroscopy confirms that all iron in the zeolite is present as ferric ions that are tetrahedrally coordinated in the framework position of the zeolite lattice. Calcination of the as-prepared zeolite at 823 K to remove the organic template induces a small fraction of framework iron to migrate to extra-framework positions, which is in agreement with our previous result [13]. Compelling evidence for the presence of extra-framework iron after calcination is the increase in quadrupole splitting of the high-spin Fe^{3+} doublet and the increase in total resonant absorption of the spectra measured under high-

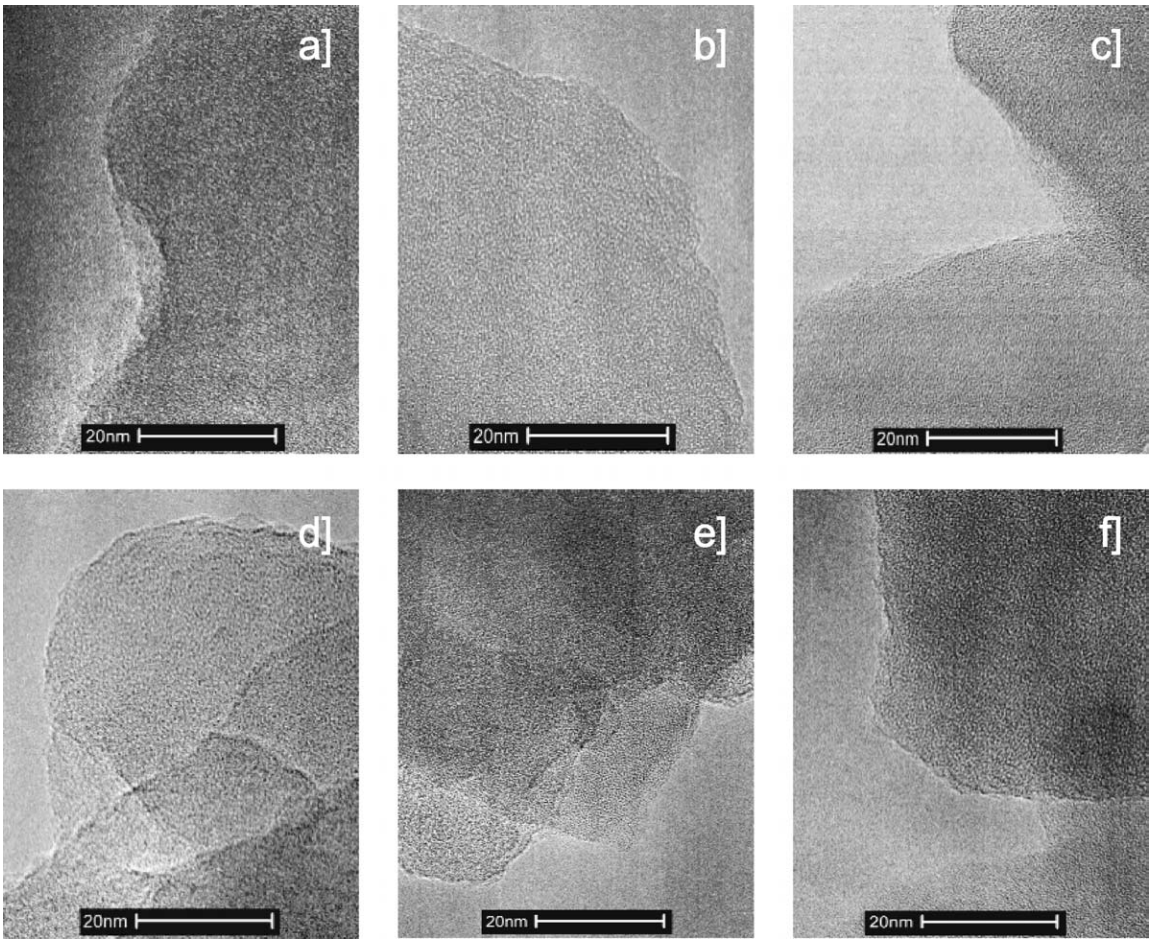

Fig. 9. TEM micrographs of steam-treated [Fe,Al]MFI zeolites: (a) [Fe,Al]MFI (1:32)$_{stm}$, (b) [Fe,Al]MFI (1:16)$_{stm}$, (c) [Fe,Al]MFI (1:8)$_{stm}$, (d) [Fe,Al]MFI (1:4)$_{stm}$, (e) [Fe,Al]MFI (1:2)$_{stm}$, and (f) [Fe,Al]MFI (1:0)$_{stm}$.

vacuum conditions. The increase in quadrupole splitting can be interpreted as an increase in electron spin interaction caused by the movement of extra-framework iron closer to other iron in both the framework and extra-framework positions. In addition, the increase in quadrupole splitting is also likely due to the presence of distorted octahedrally coordinated Fe ions in the extra-framework positions. Nonetheless, since the average isomer shift (0.54 mm s^{-1}) of the calcined sample recorded at room temperature in air is close to the isomer shift of the as-prepared sample (0.52 mm s^{-1}), the majority of the iron ions (> 80%) are still tetrahedrally coordinated in isolated framework positions. Based on the spectral contribution of the high-spin Fe^{3+} doublet and its quadrupole splitting, it appears that iron is most likely to migrate from framework to extra-framework positions during calcination if the iron and aluminum concentrations are high.

4.2. H-form [Fe,Al]MFI zeolites

Transformation of the calcined zeolites to their H-forms induces further changes on the zeolite, as deduced from the Mössbauer spectra. It is evident from the above results that transformation to the H-form of [Fe,Al]MFI (1:4) induces further migration of Fe^{3+} ions from framework to extra-framework positions, some of which are present in the reduced Fe^{2+} state. It has been shown [21–25] that extra-framework iron is able to undergo self-reduction of Fe^{3+} to Fe^{2+} ions upon heat treatment in an inert atmosphere or vacuum, in a process called “autoreduction.” However, the extent to which extra-framework iron is present as high-spin Fe^{2+} ions appears to be a function of the iron and aluminum concentrations, as illustrated in Fig. 7. As mentioned earlier, the relative intensity of the high-spin Fe^{2+} doublet appears to increase to an optimum with the decrease in iron concentration (see also Table 3). A possible explanation for this observation could be that for the zeolites with the lower iron concentration the extra-framework iron ions are mainly present as isolated species. From earlier work, we know that the smaller iron species in the MFI zeolites are the ones that reduce most readily [26]. Thus, the high-spin Fe^{2+} ions appear to increase to an optimum with the decrease in iron concentration. However, for the zeolite with the lowest iron concentration (i.e., [Fe,Al]MFI (1:32)$_H$) hardly any reduction to Fe^{2+} is observed. This indicates the necessity for at least one neighboring Fe^{3+} ion to form dimers, which would

then autoreduce in a way similar to what has been suggested for Cu^{2+} ions [27,28].

For samples with varying aluminum concentration, the spectral contribution of the high-spin Fe^{2+} doublet diminishes with the decrease in aluminum concentration and evidently is not present for [Fe,Al]MFI $(1{:}0)_H$ that contains no aluminum. This could imply that the presence of aluminum either promotes the autoreduction of Fe^{3+} ions to Fe^{2+} (in the H-form), or the lack thereof enhances the stability of framework iron against migration to extra-framework positions.

4.3. Steam-treated [Fe,Al]MFI zeolites

Steam treatment of isomorphously substituted [Fe,Al]MFI has been shown to have a profound influence on the catalyst activity in the selective oxidation of benzene to phenol and N_2O decomposition [29,30]. It has been shown [13] that steam treatment of [Fe,Al]MFI leads to complete removal of Fe^{3+} ions from the zeolite framework, which form mononuclear and small oligonuclear oxo-iron complexes, where a small fraction of Fe^{3+} was reduced to the divalent state, and larger iron oxide particles ca. 2 nm in diameter.

It is remarkable that [Fe,Al]MFI $(1{:}4)_{stm}$, [Fe,Al]MFI $(1{:}8)_{stm}$, [Fe,Al]MFI $(1{:}16)_{stm}$, and [Fe,Al]MFI $(1{:}32)_{stm}$ contain almost exclusively Fe^{2+} ions after steam treatment. Since hardly any divalent iron was observed in previous studies [11,13], this emphasizes the importance of the steaming conditions for the final state of the catalyst. For the method presented here, steam treatment of [Fe,Al]MFI with iron concentration of $\leqslant 0.6$ wt% leads to a complete removal of iron from framework to extra-framework positions, of which 90% is reduced to Fe^{2+}. This could be essential in the benzene-to-phenol reaction, since the presence of Fe^{2+} in the starting material has been correlated [1] with the formation of the active sites in the [Fe,Al]MFI catalyst.

The parameters of the high-spin Fe^{2+} doublet are strikingly similar to those reported by Panov and co-workers [31], which they assigned to binuclear iron complexes similar to those present in methane monooxygenase (MMO), for which almost equal Mössbauer parameters have been obtained [32]. In MMO the iron sites are identical, meaning that the iron ions should give fully identical components in the Mössbauer spectra. However, we observed that the high-spin Fe^{2+} doublet splits up in different components upon exposure to different gases (He or N_2) [26], thus implying that the Fe^{2+} sites in the [Fe,Al]MFI catalysts are not identical. In other words, we strongly doubt the conclusion by Panov and co-workers that the active sites resemble the iron sites in MMO.

We have stated earlier that the presence of Fe^{2+} in the starting material could be essential to the benzene-to-phenol conversion. If we assume that the catalytic performance of the [Fe,Al]MFI is related to the quantity of Fe^{2+} as proposed [1], then the presence of aluminum could be vital to the formation of these active sites, which is in agreement to the proposition of Hensen and co-workers [33]. They have shown that the performance of Fe-substituted silicalite-1 (similar to [Fe,Al]MFI $(1{:}0)_{stm}$) in the benzene-to-phenol conversion becomes substantial only after a post-synthesis dispersion of aluminum. Our work in this field (structure–activity relationship) is currently in progress and will be the subject of our next publication.

5. Conclusion

From the Mössbauer data, we have shown that iron in the as-synthesized [Fe,Al]MFI zeolites is present as paramagnetic Fe^{3+} ions that are tetrahedrally coordinated in the MFI framework regardless of iron and aluminum concentrations. Calcination of the as-synthesized [Fe,Al]MFI zeolites causes part of the framework iron to migrate into extra-framework positions. The extent of migration is more pronounced in samples with high iron and aluminum concentrations. Transformation to the H-form of the calcined [Fe,Al]MFI induces further migration of iron from framework to extra-framework positions. [Fe,Al]MFI with a very low iron content (< 0.6 wt%) tends to have Fe^{3+} ions in isolated extra-framework positions that are easily reduced to its divalent state. In addition, the presence of aluminum enhances the formation of Fe^{2+} ions. Finally, steam treatment of [Fe,Al]MFI completely removes iron from framework to extra-framework positions. All steam-treated [Fe,Al]MFI samples with ca. 1.1 wt% aluminum contain iron exclusively in the divalent state. In the steam-treated [Fe,Al]MFI, however, with low aluminum contents, the quantity of the trivalent iron increases. Since the presence of Fe^{2+} was correlated with the formation of α-sites that was claimed to be responsible for the direct oxidation of benzene to phenol [1], it appears that the presence of aluminum is essential for the formation of active iron sites in the [Fe,Al]MFI catalyst. These samples will therefore form an excellent basis for structure-activity relation studies of the direct oxidation of benzene to phenol with N_2O.

Furthermore, the absence of iron oxide particles (which are known to be spectator species in the direct oxidation of benzene to phenol with N_2O), in the steamed and specifically in the calcined and H-form samples, affirms that the relaxation behavior of iron at low temperatures (77 K and 4.2 K) in the Mössbauer spectra is caused by paramagnetic hyperfine splitting rather than superparamagnetic iron-oxided particles. This illustrates very well the complementary nature of TEM and Mössbauer spectroscopy.

Acknowledgments

Thanks to Prof. Dr. G.J. Kearley, Department of Radiation, Radionuclides and Reactors, Faculty of Applied Sciences, Delft University of Technology, for his inputs during

discussions and to Ing. M.P. Steenvoorden, for his assistance during Mössbauer measurements.

References

[1] K.A. Dubkov, N.S. Ovanesyan, A.A. Shteinman, E.V. Starokon, G.I. Panov, J. Catal. 207 (2002) 341.
[2] A.A. Battiston, J.H. Bitter, D.C. Koningsberger, Catal. Lett. 66 (2000) 75.
[3] L.J. Lobree, I. Hwang, J.A. Reimer, A.T. Bell, Catal. Lett. 63 (1999) 233.
[4] H.-Y. Chen, T. Voskoboinikov, W.M.H. Sachtler, J. Catal. 180 (1998) 171.
[5] X. Feng, W.K. Hall, J. Catal. 166 (1997) 368.
[6] E.M. El-Malki, R.A. van Santen, W.M.H. Sachtler, J. Catal. 196 (2000) 212.
[7] F. Kapteijn, G. Marbán, J. Rodríguez-Mirasol, J.A. Moulijn, J. Catal. 167 (1997) 256.
[8] G.I. Panov, Cattech 4 (2000) 18.
[9] G.I. Panov, A.K. Uriarte, M.A. Rodkin, V.I. Sobolev, Catal. Today 41 (1998) 365.
[10] P.P. Notté, Top. Catal. 13 (2000) 387.
[11] A. Ribera, I.W.C.E. Arends, S. de Vries, J. Pérez-Ramírez, R.A. Sheldon, J. Catal. 195 (2000) 287.
[12] G.I. Panov, V.I. Sobolev, A.S. Kharitonov, J. Mol. Catal. 61 (1990) 85.
[13] J. Pérez-Ramírez, G. Mul, F. Kapteijn, J.A. Moulijn, A.R. Overweg, A. Doménech, A. Ribera, I.W.C.E. Arends, J. Catal. 207 (2002) 113.
[14] N.N. Greenwood, T.C. Gibb, Mössbauer Spectroscopy, Chapman and Hall, London, 1971, Chap. 3.
[15] J.B. Taboada, A.R. Overweg, M.W.J. Crajé, I.W.C.E. Arends, G. Mul, A.M. van der Kraan, Micropor. Mesopor. Mater. 75 (2004) 237.
[16] A. Meagher, V. Nair, R. Szostak, Zeolites 8 (1988) 3.
[17] R.L. Garten, W.N. Delgass, M. Boudart, J. Catal. 19 (1970) 90.
[18] S. Mørup, J.E. Knudsen, M.K. Nielsen, G. Trumpy, J. Chem. Phys. 76 (1976) 65.
[19] S. Yuen, Y. Chen, J.E. Kubsh, J.A. Dumesic, N. Topsøe, H. Topsøe, J. Phys. Chem. 86 (1982) 3022.
[20] S. Bordiga, R. Buzzoni, F. Geobaldo, C. Lamberti, E. Giamello, A. Zecchina, G. Leofanti, G. Petrini, G. Tozzola, J. Catal. 158 (1996) 486.
[21] R. Joyner, M. Stockenhuber, J. Phys. Chem. B 103 (1999) 5963.
[22] L.J. Lobree, I. Hwang, J.A. Reimer, A.T. Bell, J. Catal. 186 (1999) 242.
[23] G. Spoto, A. Zecchina, G. Berlier, S. Bordiag, M.G. Clerici, L. Basini, J. Mol. Catal. A 158 (2000) 107.
[24] K. Lázár, A.N. Kotasthane, R. Fejes, Catal. Lett. 57 (1999) 171.
[25] T.V. Voskoboinikov, H.-Y. Chen, W.M.H. Sachtler, Appl. Catal. B 19 (1998) 279.
[26] A.R. Overweg, M.W.J. Crajé, A.M. van der Kraan, I.W.C.E. Arends, A. Ribera, R.A. Sheldon, J. Catal. 223 (2004) 262.
[27] M. Iwamoto, H. Yahiro, K. Tanda, N. Mizuno, Y. Mine, S. Kagawa, J. Phys. Chem. 95 (1991) 3727.
[28] H.-J. Jang, W.K. Hall, J.L. d'Itri, J. Phys. Chem. 100 (1996) 9416.
[29] A.S. Kharitonov, G.I. Panov, G.A. Sheveleva, L.V. Pirutko, T.P. Voskresenskaya, V.I. Sobolev, US Patent 5,672,777, 1997, assigned to Monsanto.
[30] L.V. Pirutko, V.S. Chernyavsky, A.K. Uriarte, G.I. Panov, Appl. Catal. A 227 (2002) 143.
[31] N.S. Ovanesyan, A.A. Shteinman, K.A. Dubkov, V.I. Sobolev, G.I. Panov, Kinet. Catal. 39 (1998) 792.
[32] J.G. DeWitt, J.G. Bentsen, A.C. Rosenzweig, B. Hedman, J. Green, S. Pilkington, G.C. Papaeftymiou, H. Dalton, K.O. Hodgson, S.J. Lippard, J. Am. Chem. Soc. 113 (1991) 9219.
[33] E.J.M. Hensen, Q. Zhu, R.A. van Santen, J. Catal. 220 (2003) 260.